*J. Anat.* (1991), **176**, 139–156
*With 7 figures*
*Printed in Great Britain*



# Morphometry of the human thigh muscles. A comparison between anatomical sections and computer tomographic and magnetic resonance images*

C. M. ENGSTROM, G. E. LOEB†, J. G. REID‡, W. J. FORREST AND L. AVRUCH§

*Department of Anatomy, Queen's University, † Biomedical Engineering Unit, Queen's University, ‡ School of Physical Education and Health, Queen's University and §Magnetic Resonance Unit, Ottawa General Hospital, Ottawa*

(*Accepted* 10 *December* 1990)

## INTRODUCTION

Researchers have commonly relied on muscle morphometry in studies on the mechanics of human movement. For example, a direct relationship between a muscle's cross-sectional area (CSA) and its ability to generate force has been a fundamental hypothesis for numerous biomechanical studies concerned with empirical (Fick, 1910; Franke, 1920; Haxton, 1944) or mathematical descriptions of muscle function (An, Kaufman & Chao, 1989; Crowninshield & Brand, 1981). Traditionally, researchers have obtained such morphometric data from cadaveric specimens and extrapolated these measurements to live subjects for investigating the dynamics of force production during motor tasks. However, an increasing number of studies have utilised non-invasive imaging techniques for direct, *in vivo* muscle morphometry circumventing many of the inherent limitations of cadaveric data (Ikai & Fukunaga, 1968; Maughan & Nimmo, 1984; Narici *et al.* 1989).

Ultrasound (US) was the first imaging technique used for direct measurement of muscle size in living human subjects (Ikai & Fukunaga, 1968, 1970). Researchers have continued to use this non-ionising imaging modality, particularly for obtaining morphometric data on large, superficial muscle groups (Round & Edwards, 1983; Häkkinen & Keskinen, 1989; Tabata, Atomi, Kanehisa & Miyashita, 1990). However, US procedures have limited resolution and reduced precision for controlling slice thickness and orientation compared to more recent imaging techniques.

Computer tomography (CT) has been used extensively for morphometric studies on the human musculoskeletal system. The increased resolution of muscle morphology provided in CT, as opposed to US, has been used for numerous studies on the CSA of muscle units in the lower limb (Maughan, Watson & Weir, 1983*a*, *b*), Klitgaard *et al.* 1990; Lorentzon *et al.* 1988), upper limb (Schantz *et al.* 1983; Davies, Parker, Rutherford & Jones, 1988; Alway, Stray-Gundersen, Grumbt & Gonyea, 1990) and trunk (Reid, Costigan & Comrie, 1987; McGill, Pratt & Norman, 1988). However, CT has not been used for highly detailed, serial investigations of large body structures such as whole limbs in healthy subjects due to the significant exposure to ionising radiation that would be involved with these procedures.

* Reprint requests to G. E. Loeb, Biomedical Engineering Unit, Abramsky Hall, Queen's University, Kingston, Ontario, Canada, K7L 3N6.

Table 1. *Physical characteristics of cadavers and muscle abbreviations*

| | Age (yr) | Mass (kg) | Height (m) | Cause of death |
|---|---|---|---|---|
| Cadaver 1 | 60 | 85 | 1·72 | Myocardial infarct |
| Cadaver 2 | 79 | 95 | 1·80 | Cerebral vascular accident |
| Cadaver 3 | 59 | 112 | 1·79 | Myocardial infarct |

| Abbr.* | Muscle | Abbr.* | Muscle |
|---|---|---|---|
| Sr | Sartorius | Am | Adductor magnus |
| Gr | Gracilis | Al | Adductor longus |
| St | Semitendinosus | Ab | Adductor brevis |
| Sm | Semimembranosus | Vm | Vastus medialis |
| Bfl | Biceps femoris (long head) | Vi | Vastus intermedius |
| | | Vl | Vastus lateralis |
| Bfs | Biceps femoris (short head) | Rf | Rectus femoris |

* Abbreviations for muscle names.

More recently, MR has been used to quantify muscle dimensions (Reid & Costigan, 1987; Narici, Roi & Landoni, 1988; Kariya *et al.* 1989; Narici *et al.* 1989; Tracy *et al.* 1989). In general, the MR images of soft tissue structures, such as individual muscles, are more detailed than images from other imaging techniques. As a consequence, MR has been used to calculate the CSA of individual muscles at several sites along their lengths (cf. Narici *et al.* 1989; Tracy *et al.* 1989), whereas only a very limited number of CT and US studies have generated data for individual muscles (Bulcke, Termote, Palmers & Crolla, 1979; Hudash *et al.* 1985; Ryushi, Häkkinen, Kauhanen & Komi, 1988; Sambrook, Rickards & Cumming, 1988). In addition to the highly detailed muscle morphology obtained in MR cross-sections, the resolution of bone and connective tissues appears to be adequate for calculating moment arm lengths in various muscle groups in the sagittal plane (Tracy *et al.* 1989; Rugg, Gregor, Mandelbaum & Chiu, 1990).

Magnetic resonance appears to be a promising non-invasive, non-ionising method for acquiring high resolution, multiplanar muscle morphometry for both empirical and mathematical studies concerned with the biomechanics of the human musculoskeletal system. Indeed, MR seems ideally suited for extensive and longitudinal studies in healthy human subjects. However, to be useful, the validity and limitations of morphometric data from MR, relative to other morphometric techniques, must be established through systematic, quantitative studies. The present study examines the relative accuracy and precision for MR and CT measures of the anatomical (AN) CSA of individual thigh muscles.

## MATERIALS AND METHODS

### *Cadaveric specimens*

Table 1 summarises the characteristics of the three male cadavers used in this study; it also lists abbreviations for the individual muscles from which CSA measurements were obtained using the AN, CT and MR techniques. The cadavers were fixed in a supine position using standard procedures. The pelvis was separated by a mid-sagittal section and the right lower extremities mounted individually in wooden braces to ensure a consistent orientation of the limb throughout all phases of the study. Cross-

struts and fluid filled (5 mM copper sulphate) tubes on the braces served as reference markers to facilitate data collection and analysis.

### *Morphometric procedures*

Initially, standard soft-tissue MR (Siemens, 1·5T) and CT (Toshiba 900S) imaging protocols were used to generate serial, contiguous cross-sections (10 mm thick) from a 40 cm length of the thigh superior to the lateral epicondyle. The internal laser systems of the imaging units were used to align scan series to a central cross-strut on the braces. Images were displayed as a $256 \times 256$ (MR) or $512 \times 512$ (CT) matrix and printed at $\approx 75\%$ life size on X-ray film. The specimens (including wooden braces) were then frozen solid in liquid nitrogen and transversely sectioned at 10 mm intervals with a high-speed bandsaw at levels corresponding to the mid-points of the image cross-sections. Each slice was immediately cleaned with a light spray of water and macrophotographed with a 35 mm camera.

Outlines of individual structures at each level were manually traced from the AN (life size), CT and MR records and these were enlarged onto cardboard sheets at 150% life size for final computerised planimetry. The cardboard sheets were taped to the surface of a digitising tablet where the circumferences of structures were manually traced using a stylus and, after appropriate scaling, the CSA values for individual structures were recorded in a spreadsheet. Calibration measurements conducted on a series of circles ranging from 50 to 70 $mm^2$ in area showed digitising errors to be less than 2% using the above procedures. Tendon area calculations were excluded from the final analysis due to the difficulty in consistently outlining their fuzzy boundaries in the image sections and accurately digitising their small CSAs ($\approx$ 10 to 20 $mm^2$). Figure 1 shows a set of corresponding cross-sections from the thigh mid-region.

Two independent series of measurements were made from the AN, CT and MR cross-sections: the first to examine the validity of the image-based measures with respect to the AN standard and the second to establish the retest reliability of the MR and CT measurements. The validation measurements, performed by the one operator, were conducted from a series of tracings obtained using all the AN, CT and MR records simultaneously to guide the initial identification of muscle boundaries in the cross-sections from a given limb. In contrast, reliability measurements were performed blind; the same operator, 2–3 months later, repeated the morphometric procedures for the MR and CT records having reference to only one set of image records at a time. These retest data were then compared with the original image-based measurements to establish the reliability of the techniques when performed blind; this situation more closely simulates the conditions encountered for morphometric studies with live subjects.

### *Statistical analyses*

Two statistical analyses were performed to cross-validate the corresponding AN, CT and MR measurements. Firstly, the relative accuracy of the CSA measures for all individual structures at all section levels was determined by calculating ratios between the three measurement techniques (a ratio of 1·0 indicates agreement between the paired measurements). Secondly, the relative precision between the methods for measuring the CSA of individual muscles was assessed using linear regression. Graphical representations, including ratio histograms, line graphs and scatter plots of the raw data and residuals from the regression analyses, were also used to help identify variability or systematic biases in the data detected by the numerical analyses.

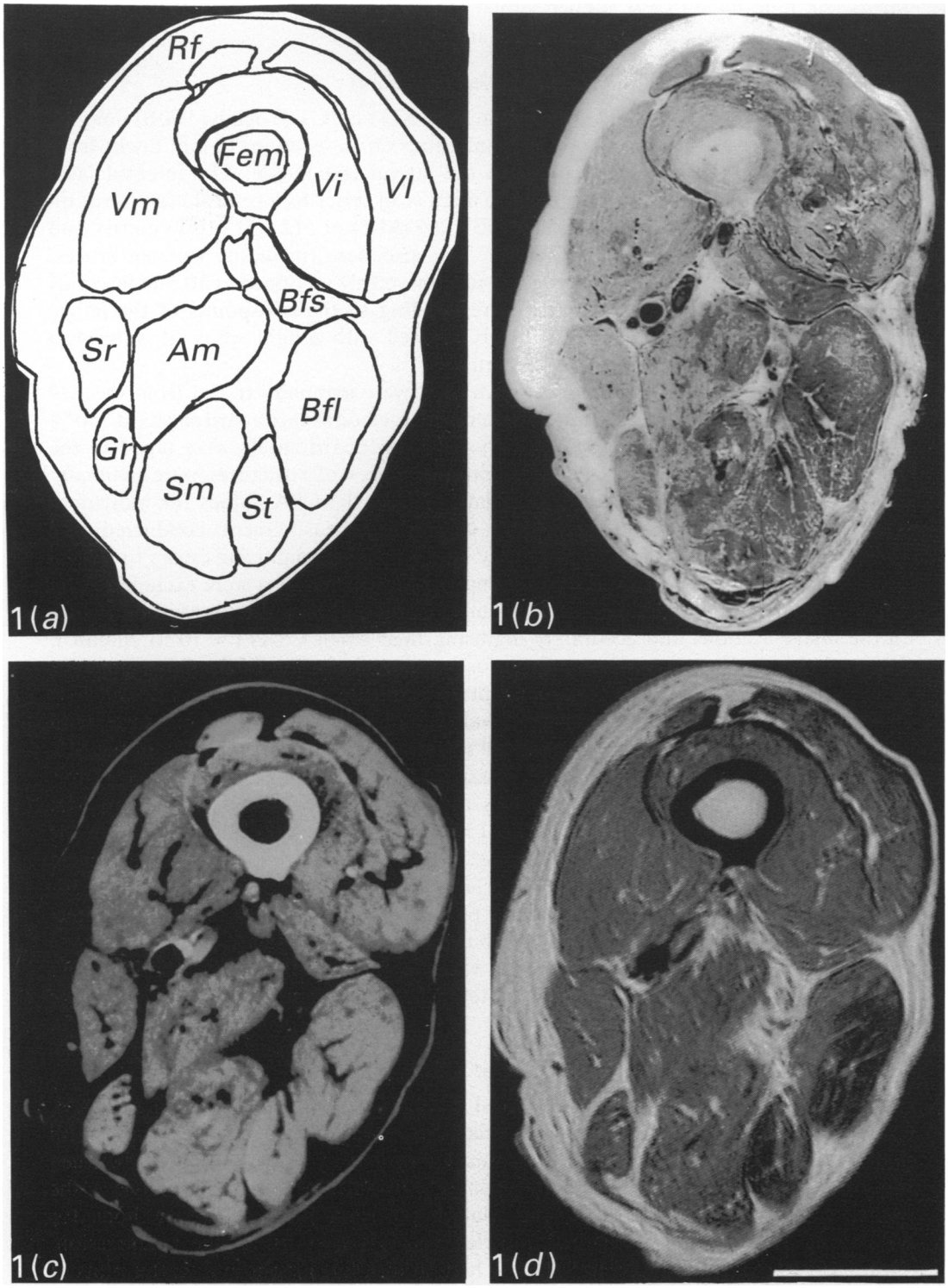


Fig. 1(*a–d*). Corresponding (*a*) digitised, (*b*) AN, (*c*) CT and (*d*) MR cross-sections from mid-thigh region (Bar, 5 cm).

Table 2. *Ratio data from measurements with recourse to all AN, CT and MR cross-sections**

| | Cadaver 1 | | | Cadaver 2 | | | Cadaver 3 | | |
|---|---|---|---|---|---|---|---|---|---|
| | MR/AN | CT/AN | CT/MR | MR/AN | CT/AN | CT/MR | MR/AN | CT/AN | CT/MR |
| Sr | 0·89±0·07 | 0·95±0·07 | 1·10±0·08 | 1·08±0·07 | 1·16±0·10 | 1·07±0·06 | 0·99±0·08 | 1·22±0·13 | 1·24±0·09 |
| Gr | 0·91±0·08 | 0·99±0·06 | 1·12±0·09 | 1·00±0·10 | 1·13±0·08 | 1·14±0·12 | 0·92±0·06 | 1·19±0·09 | 1·31±0·09 |
| St | 0·97±0·09 | 1·04±0·04 | 1·07±0·17 | 0·93±0·13 | 1·05±0·09 | 1·16±0·13 | 0·84±0·10 | 1·03±0·07 | 1·25±0·12 |
| Sm | 0·91±0·09 | 0·95±0·11 | 1·03±0·08 | 1·06±0·13 | 1·12±0·11 | 1·09±0·11 | 1·04±0·24 | 1·29±0·28 | 1·23±0·12 |
| Bfl | 0·95±0·10 | 0·95±0·07 | 1·01±0·06 | 0·96±0·26 | 1·05±0·15 | 1·16±0·12 | 0·85±0·12 | 1·08±0·08 | 1·28±0·22 |
| Bfs | 0·93±0·11 | 0·96±0·11 | 1·05±0·12 | 1·12±0·28 | 1·09±0·23 | 1·01±0·14 | 1·09±0·16 | 1·24±0·16 | 1·16±0·13 |
| Am | 1.01±0·22 | 0·91±0·10 | 0·96±0·11 | 0·95±0·10 | 1·06±0·08 | 1·14±0·09 | 0·90±0·08 | 1·10±0·12 | 1·23±0·12 |
| Al | 0·96±0·11 | 1·05±0·14 | 1·13±0·05 | 1·10±0·11 | 1·17±0·20 | 1·05±0·21 | 0·96±0·12 | 1·09±0·11 | 1·12±0·10 |
| Ab† | 1·01±0·09 | — | — | 1·06±0·10 | — | 1·29±0·15 | 1·28±0·24 | 0·99±0·38 | 0·73±0·38 |
| Vm | 0·94±0·11 | 0·99±0·06 | 1·06±0·05 | 1·06±0·13 | 1·11±0·09 | 1·06±0·10 | 1·06±0·11 | 1·19±0·09 | 1·17±0·10 |
| Vi‡ | 0·97±0·13 | 1·11±0·08 | 1·18±0·14 | 1·04±0·14 | 1·00±0·06 | 0·98±0·13 | 0·99±0·09 | 1·06±0·06 | 1·02±0·04 |
| Vl‡ | 1.02±0·14 | 0·93±0·09 | 0·93±0·13 | 1·06±0·14 | 1·03±0·08 | 0·99±0·10 | 0·88±0·10 | 0·99±0·08 | 1·22±0·14 |
| Rf | 0·96±0·08 | 0·97±0·04 | 1·04±0·12 | 1·03±0·07 | 1·22±0·07 | 1·18±0·07 | 1·00±0·05 | 1·10±0·07 | 1·10±0·05 |
| **Ag§** | **0·95±0·12** | **0·98±0·10** | **1·06±0·12** | **1·03±0·15** | **1·10±0·13** | **1·09±0·13** | **0·97±0·15** | **1·14±0·16** | **1·20±0·15** |

* Mean±S.D.

† Observations were typically < 5 in both CT and MR images.

‡ Delineation of Vi and Vl at all section levels was not possible in the CT series ( ≈ 15–20 observations).

§ Ag represents an aggregate ratio pooled across all muscles at all section levels.

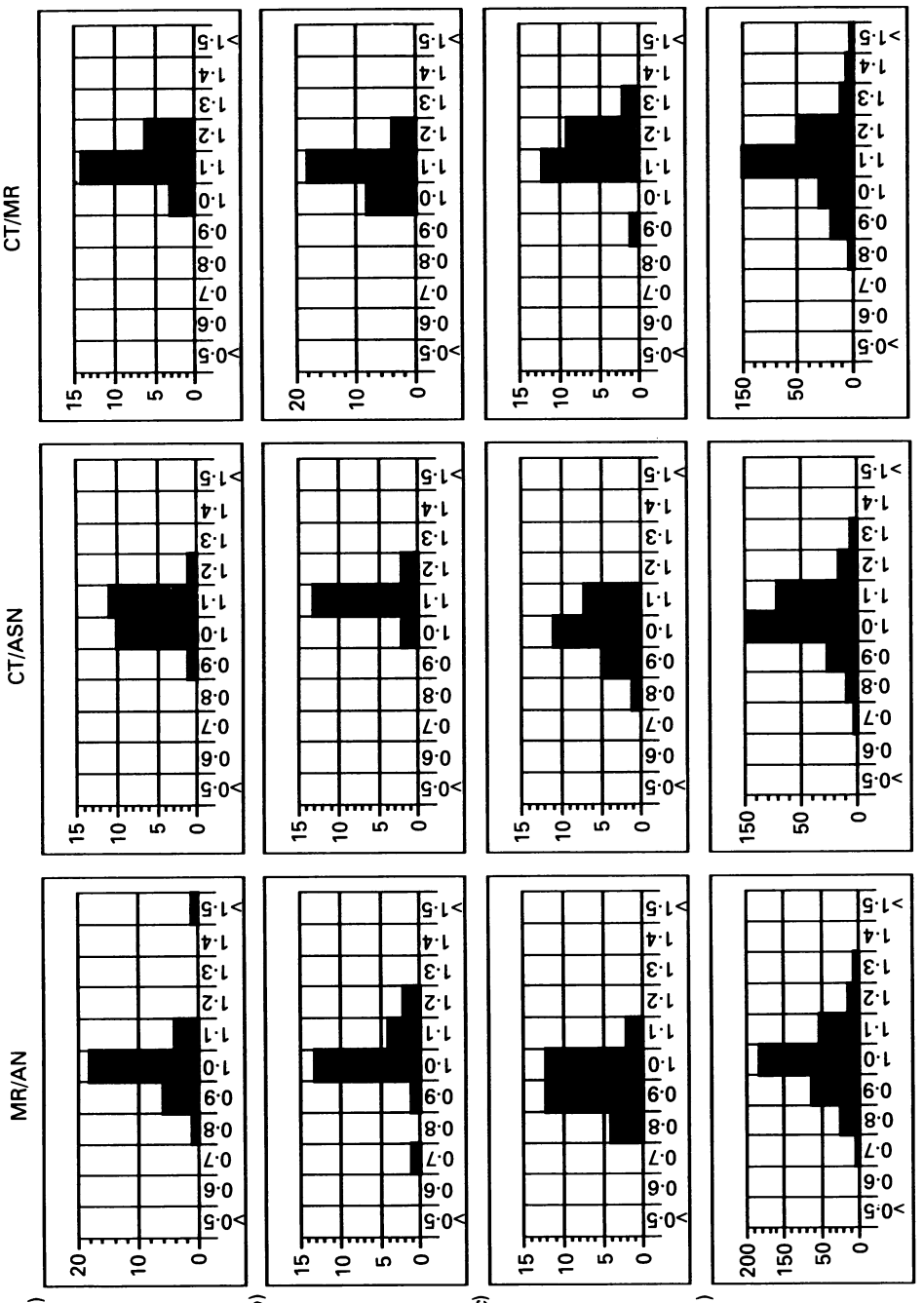


Fig. 2(*a–d*). Ratio histograms for (*a*) Vm, (*b*) St, (*c*) Sr and (*d*) aggregate data in one cadaver.

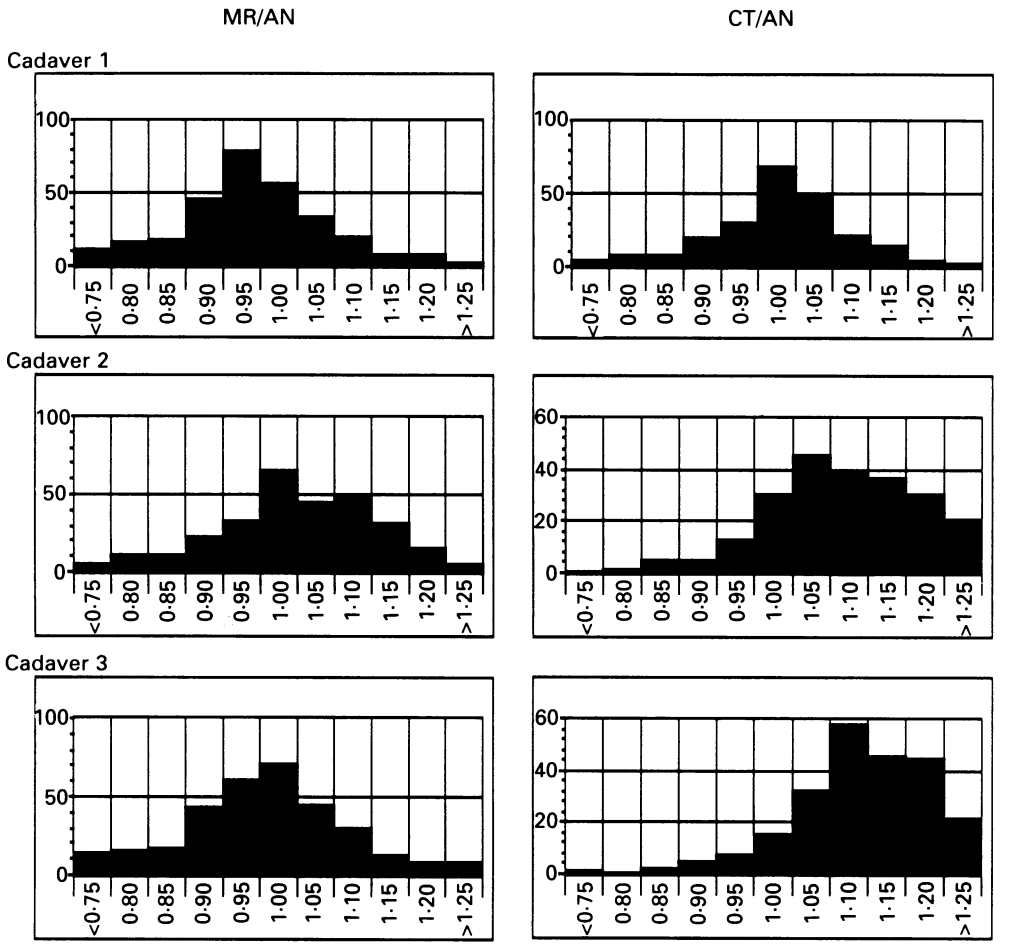


Fig. 3. Aggregate ratio histograms for all three cadavers.

### *Gross dissection*

Initial inspection of the cross-section records revealed that in the mid- to upper thigh regions, the division between Vi and Vl was not as simple or complete as first anticipated. Therefore, a further series of gross dissections was conducted on the limbs of three additional cadavers to provide (and clarify) details on the division between and the nerve supply to these two muscle bellies. Firstly, careful dissection of the nerves to Vi and Vl was performed to determine innervation patterns for these muscles. Subsequently, the extent of a septum between the two muscles was assessed by transversely sectioning Vi and Vl in 5 mm increments. The sectioning progressed from the distal to proximal extents of both muscles and, in contrast to the AN sections used for CSA measurements, was performed with a sharp knife on unfrozen muscles.

## RESULTS

### *Validation of imaging techniques*

Table 2 contains the ratio data for the first series of measurements conducted with recourse to all the AN, CT and MR cross-sections. The aggregate MR/AN ratios for

Table 3. *Correlation coefficients between paired AN, CT and MR data with recourse to all three series of cross-section records*

| | Cadaver 1 | | | Cadaver 2 | | | Cadaver 3 | | |
|---|---|---|---|---|---|---|---|---|---|
| | MR/AN | CT/AN | CT/MR | MR/AN | CT/AN | CT/MR | MR/AN | CT/AN | CT/MR |
| Sr | 0·85 | 0·84 | 0·87 | 0·95 | 0·91 | 0·96 | 0·85 | 0·76 | 0·81 |
| Gr | 0·97 | 0·99 | 0·99 | 0·98 | 0·99 | 0·98 | 0·99 | 0·98 | 0·99 |
| St | 0·99 | 1·00 | 0·99 | 0·97 | 0·98 | 0·99 | 0·99 | 1·00 | 0·99 |
| Sm | 0·99 | 0·98 | 0·99 | 0·99 | 1·00 | 0·99 | 0·99 | 0·99 | 0·99 |
| Bfl | 0·99 | 0·99 | 1·00 | 0·98 | 0·98 | 0·99 | 0·99 | 1·00 | 0·99 |
| Bfs | 0·98 | 0·99 | 0·97 | 0·95 | 0·98 | 0·95 | 0·98 | 0·98 | 0·98 |
| Am | 1·00 | 0·99 | 0·99 | 0·99 | 1·00 | 1·00 | 0·99 | 1·00 | 0·99 |
| Al | 0·98 | 0·93 | 1·00 | 0·99 | 0·97 | 0·95 | 0·95 | 0·98 | 0·99 |
| Ab | 0·98 | — | — | 0·62* | — | 0·99 | 0·98 | 1·00 | 0·79* |
| Vm | 0.99 | 0.98 | 0.99 | 0.97 | 0.97 | 0.97 | 0.99 | 0.99 | 0.99 |
| Vi | 0.96 | 0.99 | 0.97 | 0.99 | 0.99 | 0.99 | 0.98 | 1·00 | 1·00 |
| Vl | 0.98 | 0.99 | 0.98 | 0.97 | 0.98 | 0.99 | 0.99 | 0.99 | 0.99 |
| Rf | 0·99 | 1·00 | 0·99 | 0·99 | 1·00 | 0·99 | 1·00 | 1·00 | 0·99 |

* Not significant ($P > 0.0005$).
— Insufficient observations.

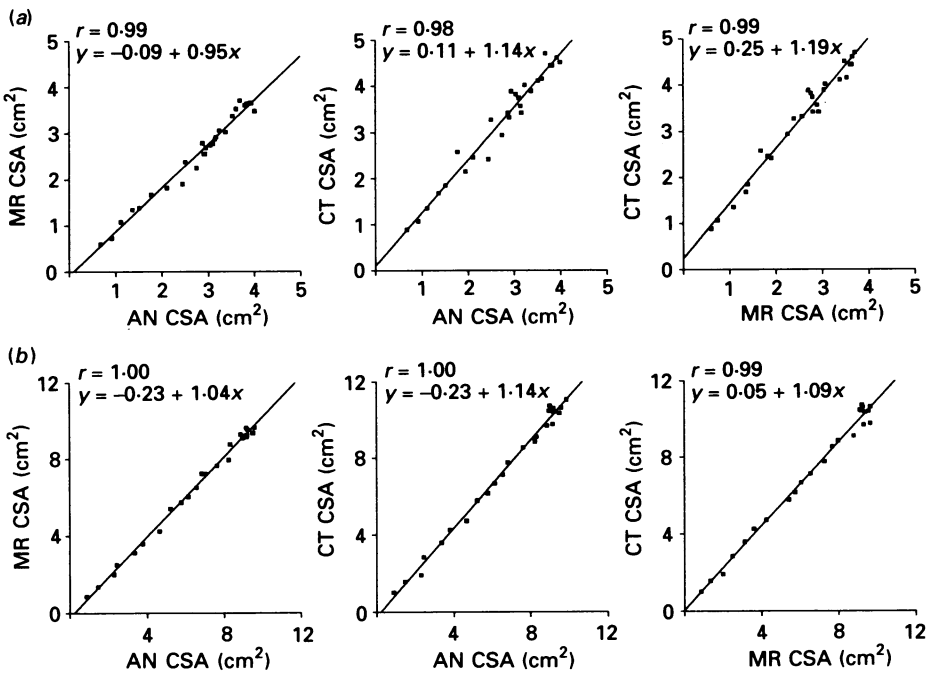


Fig. 4(*a–b*). Scatter plots of CSA measures for (*a*) Gr and (*b*) Rf in one cadaver.

all three cadavers centred around unity, with approximately 70% of the mean MR/AN ratios for individual muscles within a range of values from 0·93 to 1·07, indicating relatively high accuracy for the MR with respect to the AN standard. In contrast, aggregate CT values were not centred around the reference ratio of 1·0, suggesting that this technique was prone to errors with respect to AN CSA. The CT measures tended to overestimate muscle area by $\approx$ 10–20% compared to both AN

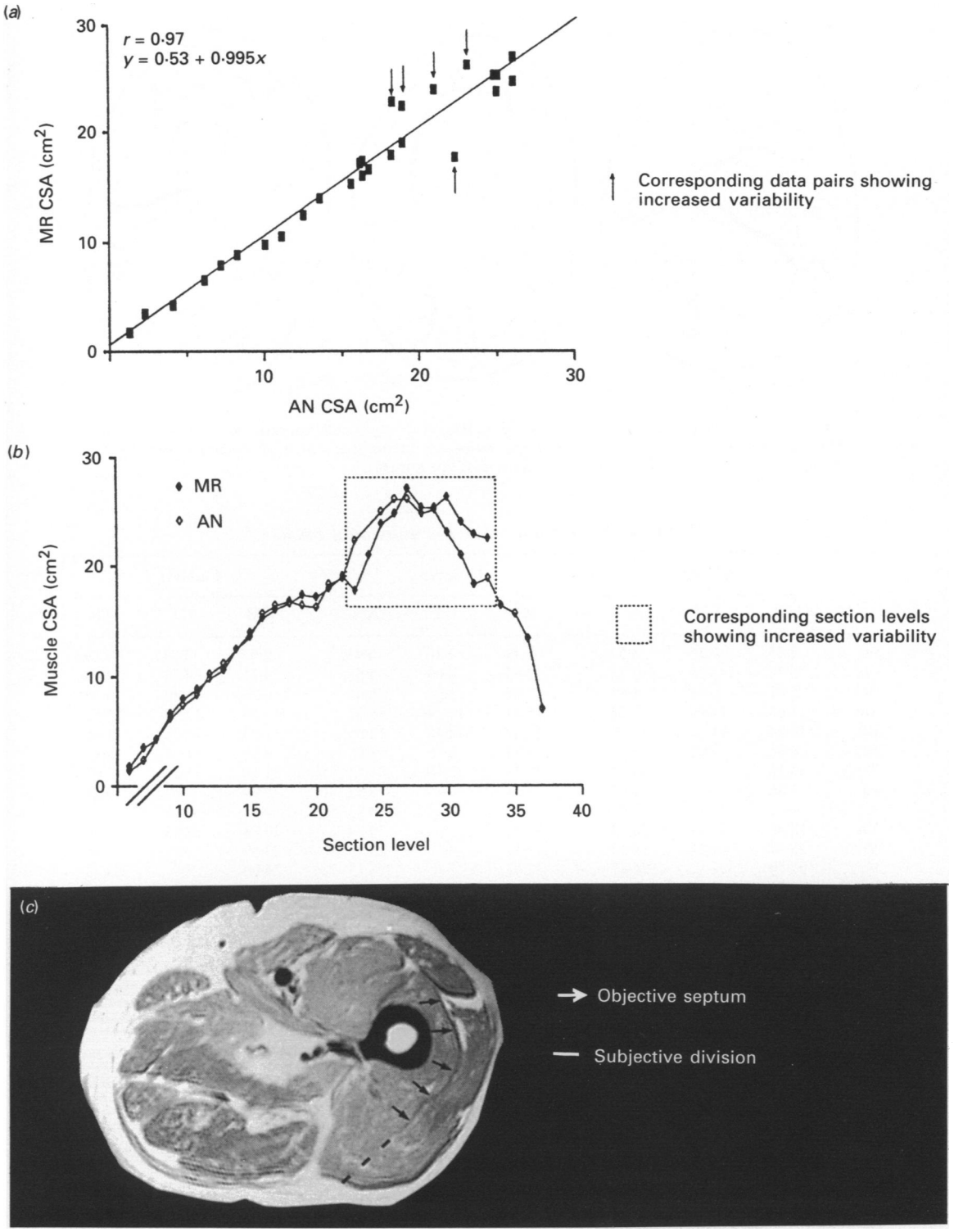


Fig. 5(*a–c*). Diagnostic techniques for isolating regions of increased variability in Vl CSA values due to subjective boundary interpretation; (*a*) scatter plot, (*b*) line graph and (*c*) MR cross-section.

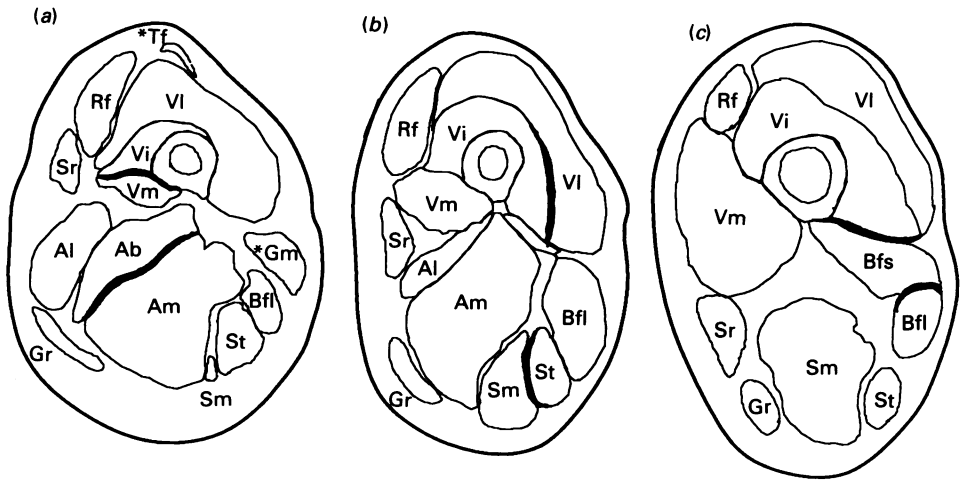


Fig. 6(*a–c*). Schematic cross-sections showing muscles with edge detection problems in (*a*) proximal, (*b*) mid- and (*c*) distal thigh cross-sections. ▬, Common sites for edge detection problems; *, tensor fasciae latae (Tf) and gluteus maximus (Gm) muscles.

Table 4. *Maximum CSA for individual muscles**

| | Cadaver 1 | | | Cadaver 2 | | | Cadaver 3 | | |
|---|---|---|---|---|---|---|---|---|---|
| | MR | CT | AN | MR | CT | AN | MR | CT | AN |
| Sr | 3·35 | 3·35 | 3·64 | 6·49 | 7·10 | 5·93 | 2·95 | 3·53 | 3·19 |
| Gr | 3·34 | 3·36 | 3·71 | 3·65 | 4·09 | 3·61 | 3·71 | 4·70 | 4·00 |
| St | 5·67 | 6·14 | 5·89 | 7·68 | 9·02 | 8·01 | 6·26 | 6·80 | 6·54 |
| Sm | 14·63 | 14·95 | 15·34 | 15·54 | 17·24 | 16·31 | 15·59 | 17·97 | 15·57 |
| Bfl | 10·84 | 11·71 | 12·08 | 13·02 | 14·40 | 13·85 | 11·03 | 12·85 | 11·66 |
| Bfs | 6·86 | 7·05 | 7·35 | 7·84 | 8·78 | 8·96 | 8·50 | 11·81 | 8·87 |
| Am | 34·16 | — | 34·81 | 28·38 | 32·18 | 31·14 | 31·10 | 35·22 | 32·63 |
| Al | 11·86 | — | 12·62 | 9·28 | — | 8·53 | 9·90 | — | 9·24 |
| Ab | — | — | 17·02 | — | — | 10·33 | — | — | — |
| Vm | 18·48 | 19·41 | 20·04 | 21·32 | 23·84 | 20·24 | 20·83 | 22·63 | 20·97 |
| Vi | 18·45 | 21·44 | 18·13 | 19·39 | — | 20·33 | 23·09 | — | 22·48 |
| Vl | 27·50 | — | 26·87 | 27·07 | — | 26·13 | 24·00 | — | 25·78 |
| Rf | 7·75 | 7·97 | 8·02 | — | — | 6·93 | 9·64 | 11·05 | 9·87 |

* CSA in $cm^2$.

— Values absent due to boundary detection problems or CT and MR sections terminated prior to section levels containing the maximum cross-section of individual muscles.

and MR, a trend more clearly seen in ratio histograms. Figure 2 shows a typical set of histograms from one cadaver; the negatively skewed distribution for the CT-based area measurements is apparent for both the individual and aggregate conditions. Figure 3 presents the aggregate ratio histograms for each of the three cadavers. The MR/AN histograms were consistently centred about 1·0; conversely the CT/AN histograms were skewed toward ratios greater than 1·0 for two of the three cadavers. Such a trend was not apparent in Cadaver 1; however, the CT images from this specimen were seriously distorted by 'air artefact' (introduced through embalming procedures) and measurements could only be obtained for $\approx$ 50% of the image series.

Comparisons with corresponding raw AN CSAs showed that both imaging techniques had good relative precision, as evidenced by the uniformly high correlation

Table 5. *Ratios from MR and CT test–retest measurements**

| | Cadaver 1 | | Cadaver 2 | | Cadaver 3 | |
|---|---|---|---|---|---|---|
| | MR/M1† | CT/C1‡ | MR/M1 | CT/C1 | MR/M1 | CT/C1 |
| Sr | 1·03 ± 0·05 | 1·01 ± 0·04 | 1·01 ± 0·04 | 1·03 ± 0·03 | 1·03 ± 0·05 | 1·00 ± 0·05 |
| Gr | 1·07 ± 0·05 | 1·03 ± 0·03 | 1·03 ± 0·05 | 1·04 ± 0·06 | 1·07 ± 0·05 | 1·00 ± 0·06 |
| St | 1·00 ± 0·03 | 1·03 ± 0·04 | 1·04 ± 0·15 | 1·01 ± 0·03 | 1·00 ± 0·03 | 1·00 ± 0·04 |
| Sm | 1·00 ± 0·06 | 0·99 ± 0·02 | 1·01 ± 0·04 | 1·06 ± 0·04 | 1·00 ± 0·06 | 1·01 ± 0·05 |
| Bfl | 0·98 ± 0·04 | 1·02 ± 0·05 | 1·01 ± 0·09 | 1·01 ± 0·05 | 0·98 ± 0·04 | 0·98 ± 0·10 |
| Bfs | 1·00 ± 0·10 | 1·01 ± 0·06 | 0·92 ± 0·14 | 0·95 ± 0·11 | 1·00 ± 0·10 | 0·92 ± 0·16 |
| Am§ | 0·96 ± 0·09 | — | 1·03 ± 0·05 | 1·05 ± 0·06 | 0·96 ± 0·09 | 0·95 ± 0·11 |
| Al | 0·97 ± 0·06 | — | 1·06 ± 0·14 | 1·09 ± 0·08 | 0·97 ± 0·06 | 1·00 ± 0·09 |
| Ab | — | — | 1·26 ± 0·38 | 1·17 ± 0·03 | — | — |
| Vm | 1·00 ± 0·04 | 1·00 ± 0·04 | 0·97 ± 0·05 | 1·00 ± 0·03 | 1·00 ± 0·04 | 0·98 ± 0·06 |
| Vi‖ | 1·01 ± 0·10 | — | 1·10 ± 0·22 | — | 1·01 ± 0·10 | 0·92 ± 0·09 |
| Vl | 1·02 ± 0·07 | — | 0·98 ± 0·04 | — | 1·02 ± 0·07 | 0·99 ± 0·10 |
| Rf | 1·02 ± 0·03 | 1·02 ± 0·03 | 1·03 ± 0·04 | 1·01 ± 0·04 | 1·02 ± 0·03 | 1·00 ± 0·02 |
| **Ag¶** | **1·01 ± 0·07** | **1·01 ± 0·04** | **1·02 ± 0·12** | **1·02 ± 0·07** | **1·01 ± 0·06** | **0·98 ± 0·08** |

* Mean ± S.D.
† M1 represents retest MR measurements.
‡ C1 represents retest CT measurements.
§ Air artefacts in CT records prevented clear definition of the adductor muscles.
‖ Delineation of Vi and Vl at all section levels was not possible in the CT series.
¶ Ag represents an aggregate ratio pooled across all muscles at all section levels.

coefficients between measurements (Table 3). Figure 4 presents a series of typical scatter plots showing good agreement between corresponding pairs of measurements over a large range of CSA values. Typically, there was an increased scatter in the data points from both tapering ends of fusiform muscles. Any departure from this general pattern (Fig. 5*a*) suggested the presence of additional sources of error, which were identified by comparing the individual CSA measurements over the length of the muscle (Fig. 5*b*) and reviewing the relevant original images (Fig. 5*c*). Figure 6 shows schematic cross-sections at three levels of the thigh where subjective interpretations of muscle boundaries were necessary for CSA calculations. Obviously, an increased need for subjective procedures increased the variability between the measurements from the three techniques (see Table 2).

Table 4 lists the maximum CSA of the individual thigh muscles in the three cadavers. These measurements were typically obtained from corresponding or immediately adjacent AN, CT and MR cross-section levels. Consistent with previous analyses, CT tended to overestimate the maximum AN CSA of individual muscles by $\approx$ 10 to 20%.

### *Gross dissections*

The results from the gross dissections showed that, in two cadavers, Vl possessed two major nerve branches: one supplying the main muscle mass and a second to a small and distinct proximal belly. Further dissection revealed little overlap between muscle regions supplied by the nerves to Vi and Vl, suggesting that they might be co-extensive with the anatomical boundaries of these muscle bellies. However, a discrete anatomical division between Vi and Vl by an intervening connective tissue septum was not observed in all of the transverse sections, particularly in the mid- to upper thigh region. Specifically, the muscle bellies were fused for about 25–35% of their length, with an incomplete posterior division. Thus, the gross dissection results confirmed and clarified the observations in the AN, CT and MR cross-sections (see also Willan,

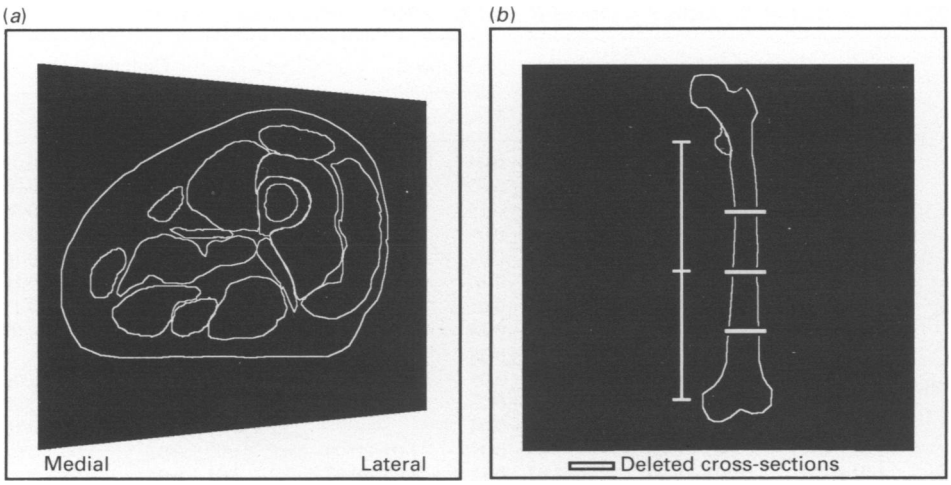


Fig. 7(*a–b*). Error sources in MR system; (*a*) pin-cushion distortion in video unit and (*b*) incorrect slice thickness requiring the removal of three MR cross-sections (Bar, extent of 40 cross-sections).

Mahon & Golland, 1990). Indeed, the variability in Vi and Vl CSA measurements for certain regions appears to be related to errors in subjectively locating borders where the septum dividing the two bellies was anatomically incomplete (Fig. 5). Interestingly, the intermuscular septum was more prominent in the MR, rather than the AN cross-sections, appearing as a uniform, dark strip in the former and a thin, intermittent line in the latter. The CT images lacked sufficient detail to delineate consistently the boundary between Vi and Vl at all section levels.

### *Reliability measurements*

For both CT and MR, the test–retest ratios were closely centred around unity (Table 5) and all the correlation coefficients between paired observations were significant with 95% of the comparisons exceeding $r = 0{\cdot}95$ ($P < 0{\cdot}0005$). In combination, these results indicate that there was good test–retest reliability for the CT and MR measurements.

### *Error sources*

In addition to the fundamental limits of precision and accuracy revealed by these analyses, two equipment-specific sources of error were identified through the systematic approach to validation adopted in this study. Initial analyses of the aggregate MR/AN ratio data and accompanying histograms revealed that CSA values were systematically over- or underestimated for structures on the medial or lateral aspects of the MR records, respectively. This medio-lateral gradient for area measurements was traced to a pin-cushion distortion in the video screen of the X-ray film processing machine used for MR hardcopy (Fig. 7*a*). After the distortion had been confirmed and corrected, the MR images were reprinted and used for the analyses presented here. In addition, visual inspection of corresponding AN and CT cross-sections in Cadaver 3 (examined one month after Cadavers 1 and 2) revealed a subtle inconsistency in the alignment between the MR and AN cross-sections. Apparently, a small calibration error in the slice-select gradient of the MR system resulted in a section interval of 9·25 mm rather than the 10 mm requested and indicated on the MR output records. This in turn, resulted in an MR series in which

the 40 sections covered 37 cm instead of the 40 cm covered by the AN and CT sections. Compensation for these alignment anomalies was obtained by deleting the three most obviously misaligned MR sections (Fig. 7*b*). Unfortunately, the lack of coverage at the most proximal regions of the limb precluded measurements of total volume for some muscles.

## DISCUSSION

Valid morphometric data on the human musculoskeletal system are important for many biomechanical analyses of motor tasks. Recently, non-invasive imaging techniques such as MR and CT have been used to quantify the CSA of human thigh muscles (Alway *et al.* 1990; Maughan *et al.* 1983*a*, *b*; Narici *et al.* 1989). Surprisingly, the relative accuracy and precision of these imaging techniques for obtaining these measurements have not been established by any systematic cross-validation with corresponding AN measures.

### *Relative merits of MR vs CT*

The present results indicated that MR provided valid measures of the AN CSA of most individual thigh muscles. In contrast, CT tended consistently to overestimate AN measures of muscle area. Hudash *et al.* (1985) have previously shown that CT generally overestimates the AN CSA of individual thigh muscles by about 10–20%. Presumably, the profiles of the muscles were enlarged at the expense of the more radiolucent surrounding tissues in the CT cross-sections; such errors might be related to the averaging and filtered back-projection procedures used for generating images with this technique (Stytz & Frieder, 1990). Magnetic resonance imaging procedures do not rely on filtered back-projection data for image reconstruction. Instead, images are generated using Fourier transformations of the nuclear magnetic resonance signals. The amplitude of this radio-frequency (RF) signal reflects the density and chemical state of the hydrogen nuclei in individual voxels whose co-ordinates in the specimen are identified by the phase and frequency of the RF signal. The correspondence between the frequency/phase space and the position of the tissue in the magnet bore is established by the interaction between RF pulsing sequences and field gradients imposed onto the static magnetic field (Shaw, 1988; cf. Edelstein, Hutchinson, Johnson & Redpath, 1980). Incorrect calibration of these field gradients is one potential source of error, particularly in the slice-select (longitudinal) axis (see Fig. 7*b* and Results).

The basic outlines of most muscles were equally well demonstrated with both imaging techniques; however, MR provided superior differentiation between muscle and connective tissues which allowed CSA calculations for certain muscle bellies not adequately resolved in CT records (see below). Indeed, the high intra-observer reliability for the MR and CT retest measurements would suggest that, after appropriate familiarisation with cross-sectional anatomy, an operator can consistently identify the profile of the individual thigh muscles in these images. Clearly, MR would be the preferred technique for detailed morphometric studies on living subjects because of its greater accuracy, superior soft-tissue resolution (Berquist, 1986; Narici *et al.* 1989) and the lack of known biological hazards associated with the technique (Saunders & Smith, 1984; Stuchly, 1990). Furthermore, MR has the potential for direct, multiplanar imaging (without repositioning the subject) which has allowed researchers to calculate moment arm lengths (another important morphometric parameter for musculoskeletal modelling) from high resolution sagittal images (Tracy *et al.* 1989; Rugg *et al.* 1990). Narici *et al.* (1989) have also suggested that fibre

pennation angle can be discerned in coronal images of the quadriceps femoris. In the present study, high contrast striations in both pennate and parallel-fibred muscles were observed in coronal and sagittal images; presumably these 'pennation angles' are defined by the fat that runs parallel to and between the muscle fascicles. However, the true compound pennation angle with respect to line of muscle pull must be calculated using trigonometric transformations and the accuracy of these estimates requires validation against cadaveric dissections (work in progress).

*Sources and corrections of MR calibration errors*

While MR appears to be the current imaging technique of choice for morphometry of the human thigh musculature, the novel cross-validation procedures used in this study highlighted several system-related calibration errors. If left uncorrected, such errors might seriously compromise the validity of biomechanical models or clinical studies based on such data. Therefore, the calibration options routinely provided for clinical imaging units should be supplemented with external reference measurements to ensure that system-related errors do not bias morphometric data. Specifically, the specimen under investigation should be placed within an orthogonal frame of precisely aligned columns (e.g. copper sulphate-filled tubes) in order to verify the absolute scale and rectangularity of the resultant image space. Obliquely orientated bars could be added to confirm the serial order of images, a concern when scans are collected in interrupted or interleaved sequences or when subjects are repositioned for multiple scan series. Two reference marks that cover the extent of the imaging series (e.g. the ends of the oblique rods) could also serve to establish the accuracy of the longitudinal spacing between sections.

Morphometric data obtained from optical-based hardcopy (e.g. photographic or X-ray film) may also be biased due to pin-cushion distortions (see Fig. 7*a* and Results) or related geometric inconsistencies in video displays. Such distortions are common in fluoroscopic units and corrections for errors in the image plane have been developed, but the methods are computationally intensive and are designed for digital as opposed to optical representations of the image (Wallace & Johnson, 1981). When morphometric data are based on pixel co-ordinates in a digital image (as opposed to physical position on a video display or print), such errors are avoided. Fortunately, the adoption of file-interchange standards for digital image formats is expediting the application of automated image handling and analysis of clinical MR images. Such techniques can be used to locate automatically and measure the calibration points in each image (Zhu, Checkley, Hickey & Isherwood, 1986) and have been applied to semi-automate the detection of anatomical boundaries (Wang, Mezrich & Sebok, 1990). However, substantial improvements in both image resolution and edge-detection algorithms will be necessary before morphometry of individual muscles can be more fully automated.

*Interpretation of muscle boundaries*

A detailed knowledge of the cross-sectional anatomy of the thigh is required for objective or informed subjective interpretations of muscle boundaries in MR images. Obviously, subjective decisions are required when muscle borders are indistinct due to an intimate connection of individual bellies or apposition of adjacent structures and this, in turn, reduces the relative measurement accuracy between image-based and AN values. For example, edge detection problems were encountered for muscles with two heads, such as Bfs and Bfl, and this decreased the accuracy between MR and AN

measurements (see Table 2). However, over most of the length of the thigh, MR images provided clearly defined boundaries for individual muscle bellies.

There are several factors that might influence boundary resolution in image-based studies of the muscles from live or cadaveric subjects. Sambrook *et al.* (1988) proposed that an increased connective tissue content in the muscles of older subjects (such as our cadavers) improved the definition between adjacent muscle units. Furthermore, Hudash *et al.* (1985) have suggested that distinguishing muscle borders in lean, athletic subjects is difficult with CT procedures and that boundary detections would be facilitated in subjects with an increased body fat percentage (common in cadaveric material). There is also the concern that chemical fixation and other postmortem changes in cadaveric materials might alter the contrast between different soft tissue structures (Bos, Verbout, Bloem & Leeuwen, 1990). However, recently published MR images of the thigh muscles from young, normal, living subjects have comparable quality to the cadaveric images obtained in the present study (cf. Narici *et al.* 1989).

Part of the variability between the AN and image-based measurements is presumably related to the fact that the CT and MR images were integrated over a 10 mm slice thickness, whereas the AN records were obtained from a single, discrete plane of section centred within this thickness. Therefore, image-based values represent an 'averaged' muscle CSA whilst AN records provide a discrete area measurement; this may account for some of the observed variability particularly at the tapering ends of the muscles. The boundary detection problems mentioned earlier were also related to this 'averaging' phenomenon. Adjacent muscle bellies were generally separated by a thin plane of connective tissue that appeared as one distinct line in the AN cross-sections. However, if this plane was not perpendicular to the plane of cross-section, it appeared as a fuzzy, sometimes intermittent, band of only slightly differing contrast to the surrounding muscle in CT and MR images.

One solution for reducing these averaging errors and increasing the definition of muscle boundaries might be to decrease the section thickness for the imaging techniques. This might also increase the resolution of tendon profiles; currently image-based morphometry on tendons has been limited to the large and easily defined Achilles tendon (Komi, Salonen, Järvinen & Kokko, 1987). However, reduced slice thickness requires increased imaging times to obtain images of similar quality to those produced from thick cross-sections. Thus, 10 mm section thickness and interval seems to offer a good compromise between accuracy and time constraints for determining the AN CSA of the human thigh muscles; it has been a commonly used slice thickness (Narici *et al.* 1988, 1989; Kariya *et al.* 1989).

Interestingly, all boundary identification problems in image-based cross-sections may not be related to the resolution of these techniques; specifically, subjective interpretations of the division between Vi and Vl were required in the present study due to an anatomically incomplete septum between these muscles (see Results: Gross dissections). Recently, Willan *et al.* (1990) performed a comprehensive series of gross dissections on Vi and Vl and reported that in about 75% of cases the division between these two muscles is apparent only for 50–75% of their length. As mentioned previously, a dividing line between the two muscles was actually more prominent in the MR, as opposed to the AN, cross-sections. A corresponding line in the CT records was apparent in only some of the sections. Indeed, Häggmark, Jansson & Svane (1979) treated Vi and Vl as one entity for CT morphometry, whereas others have usually measured the CSA of the quadriceps femoris as a whole (e.g. Lorentzon *et al.* 1988; Maughan *et al.* 1983*a*; Klitgaard *et al.* 1990). Surprisingly, Ryushi *et al.* (1988)

reported that they measured the CSA of the human Vl with US although records of the images used for these analyses or descriptions of the anatomical extents of these muscles were not provided. Narici *et al.* (1989) claimed to have accurately determined the CSA for both Vi and Vl at serial longitudinal positions using MR and made no report of an incomplete boundary in the images of these muscles.

### *Suggestions for further work*

Typically, imaging techniques have been used for CSA measurements of individual muscles at one longitudinal level in a single limb posture. Obviously, such comparisons are of limited value across subjects and are prone to alignment errors in repeated measurements from an individual over time. Indeed, the longitudinal position and magnitude of the maximal CSA that is measured for a muscle will depend on joint angle (Ikai & Fukunaga, 1968), muscle tone and shape or size of adjacent structures. However, the total volume must remain relatively constant (cf. Otten, 1988). Furthermore, volumetric data may be combined with fascicle length to produce physiological CSA (PCSA) which can be related directly to the force-generating capabilities of muscles with both pennate and parallel-fibred architectures (Close, 1972). Simple AN CSA, even if taken at the point of maximal CSA, is useful only as a predictor of relative muscle force and then only if the fibre architecture remains constant. Friederich & Brand (1990) have suggested that extrapolations from cadavers are unlikely to predict accurately the PCSAs of individual muscles in living subjects.

MR offers the possibility of calculating PCSA in living subjects, but only if two conditions are satisfied: (i) pennation angle must be accurately measured and converted trigonometrically to fascicle length (see above); and (ii) accurate semi-automated techniques must be developed to process the large number of sections required to obtain muscle volume. A more detailed physiological profile of potential muscle function is also possible with the combined use of quantitative MR spectroscopy (Kariya *et al.* 1989). Such data may be advantageous for clinical applications in which the accuracy of musculoskeletal models for individual patients is often a limiting factor in the design and control of prostheses (Bernotas, Crago & Chizeck, 1987; Yamaguchi & Zajac, 1990).

## SUMMARY

The present study examined the relative accuracy and precision of MR and CT procedures for determining the CSA of individual muscles from the human thigh. Serial AN, CT and MR cross-sections were obtained from three cadaveric lower limbs. The MR measurements provided accurate and precise values for the CSAs of most thigh muscles, generally within $\pm 7{\cdot}5\%$ of the AN standard. In contrast, CT tended systematically to overestimate the AN CSA by 10–20%. Retest procedures indicated that highly reliable measurements could be obtained from both MR and CT images. However, subjective interpretations of boundaries between closely apposed muscle bellies, particularly for muscles with more than one head, were necessary for resolving entities in the imaging records and this decreased the relative accuracy of MR and CT measures. Interestingly, MR records demonstrated an incomplete septum between vastus lateralis and vastus intermedius more prominently than AN cross-sections. The novel cross-validation procedures used in this study also highlighted several system-based errors in the MR records that, if undetected and left uncorrected, would have seriously biased the morphometric data obtained with this technique. In general, MR

provides high resolution images of the human thigh muscles which may be used to obtain valid measures of the CSA of these structures.

This work was supported by a grant from the Muscular Dystrophy Association of Canada. We are grateful to Mrs B. Arldt for performing the CT procedures and Mr R. Hunt for assistance with anatomical sectioning.

## REFERENCES

ALWAY, S. E., STRAY-GUNDERSEN, J., GRUMBT, W. H. & GONYEA, W. J. (1990). Muscle cross-sectional area and torque in resistance trained subjects. *European Journal of Applied Physiology and Occupational Physiology* **60**, 86–89.

AN, K. N., KAUFMAN, K. R. & CHAO, E. Y. S. (1989). Physiological considerations of muscle force through the elbow joint. *Journal of Biomechanics* **22**, 1249–1256.

BERNOTAS, L. A., CRAGO, P. E. & CHIZECK, H. J. (1987). Adaptive control of electrically stimulated muscle. *IEEE Transactions on Biomedical Engineering* **34**, 140–147.

BERQUIST, T. H. (1986). Magnetic resonance imaging of the extremities. *Seminars in Ultrasound, Computer Tomography and Magnetic Resonance* **7**, 320–330.

BOS, C. F. A., VERBOUT, A. J., BLOEM, J. L. & LEEUWEN, VAN M. B. M. (1990). A correlated study of MR images and cryo-sections of the neonatal hip. *Surgical and Radiological Anatomy* **12**, 43–51.

BULCKE, J. A., TERMOTE, J.-L., PALMERS, Y. & CROLLA, D. (1979). Computed tomography of the human skeletal muscular system. *Neuroradiology* **17**, 127–136.

CLOSE, R. I. (1972). Dynamic properties of mammalian skeletal muscles. *Physiological Reviews* **52**, 129–197.

CROWNINSHIELD, R. D. & BRAND, R. A. (1981). A physiologically based criterion of muscle force production in locomotion. *Journal of Biomechanics* **14**, 793–801.

DAVIES, J., PARKER, D. F., RUTHERFORD, O. M. & JONES, D. A. (1988). Changes in strength and cross sectional area of the elbow flexors as a result of isometric strength training. *European Journal of Applied Physiology and Occupational Physiology* **57**, 667–670.

EDELSTEIN, W. A., HUTCHINSON, J. M. S., JOHNSON, G. & REDPATH, T. (1980). Spin-wrap NMR imaging and applications to human whole-body imaging. *Physics in Medicine and Biology* **25**, 751–756.

FICK, R. (1910). *Handbuch der Anatomie und Mechanik der Gelenke unter Berücksichtigung der bewegenden Muskeln*. Jena: Fischer.

FRANKE, F. (1920). Die Kraftkurve menschlicher Muskeln bei willkürlicher Innervation und die Frage der absoluten Muskelkraft. *Pflügers Archiv fuer die gesamte Physiologie des Menschen und der Tiere* **184**, 300–322.

FRIEDERICH, J. A. & BRAND, R. A. (1990). Muscle fiber architecture in the human lower limb. *Journal of Biomechanics* **23**, 91–95.

HÄGGMARK, T., JANSSON, E. & SVANE, B. (1978). Cross-sectional area of the thigh muscle in man measured by computer tomography. *Scandinavian Journal of Clinical and Laboratory Investigation* **38**, 355–360.

HÄKKINEN, K. & KESKINEN, K. L. (1989). Muscle cross-sectional area and voluntary force production characteristics in elite strength trained and endurance-trained athletes and sprinters. *European Journal of Applied Physiology and Occupational Physiology* **57**, 215–220.

HAXTON, H. A. (1944). Absolute muscle force in the ankle flexors of man. *Journal of Physiology* **103**, 267–273.

HUDASH, G., ALBRIGHT, J. P., MCAULEY, E., MARTIN, R. K. & FULTON, M. (1985). Cross-sectional thigh components: computerized tomographic assessment. *Medicine and Science in Sports and Exercise* **17**, 417–421.

IKAI, M. & FUKUNAGA, T. (1968). A study on training effect on strength per unit cross-sectional area of human muscle by means of ultrasonic measurement. *Internationale Zeitschrift für angewandte Physiologie einschliesslich Arbeitsphysiologie* **26**, 26–32.

IKAI, M. & FUKUNAGA, T. (1970). Calculation of muscle strength per unit cross-sectional area of human muscle by means of ultrasonic measurement. *Internationale Zeitschrift für angewandte Physiologie einschliesslich Arbeitsphysiologie* **28**, 173–180.

KARIYA, Y., ITOH, M., NAKAMURA, T., YAGI, K. & KUROSAWA, H. (1989). Magnetic resonance imaging and spectroscopy of thigh muscles in cruciate ligament insufficiency. *Acta orthopaedica scandinavica* **60**, 322–325.

KLITGAARD, H., MORANTI, M., SCHIAFFINO, S., AUSONI, S., GORZA, L., LAURENT-WINTER, C., SCHNOHR, P. & SALTIN, B. (1990). Function, morphology and protein expression of ageing skeletal muscle: a cross-sectional study of elderly men with different training backgrounds. *Acta physiologica scandinavica* **140**, 41–54.

KOMI, P. V., SALONEN, M., JÄRVINEN, M. & KOKKO, O. (1987). *In vivo* registration of Achilles tendon forces in man. 1. Methodological development. *International Journal of Sports Medicine* **8** (*Suppl.*), 3–8.

LORENTZON, R., JOHANSSON, C., SJÖSTRÖM, M., FAGERLUND, M. & FUGL-MEYER, A. R. (1988). Fatigue during dynamic muscle contractions in male sprinters and marathon runners: Relationships between performance, electromyographic activity, muscle cross-sectional area and morphology. *Acta physiologica scandinavica* **132**, 531–536.

MAUGHAN, R. J. & NIMMO, M. A. (1984). The influence of variations in muscle fibre composition on muscle strength and cross-sectional area in untrained males. *Journal of Physiology* **351**, 299–311.

MAUGHAN, R. J., WATSON, J. S. & WEIR, J. (1983*a*). Strength and cross-sectional area of human skeletal muscle. *Journal of Physiology* **338**, 37–49.

MAUGHAN, R. J., WATSON, J. S. & WEIR, J. (1983*b*). Relationship between muscle cross-sectional area in male sprinters and endurance runners. *European Journal of Applied Physiology and Occupational Physiology* **50**, 309–318.

MCGILL, S. M., PRATT, N. & NORMAN, R. W. (1988). Measurement of the trunk musculature of active males using CT scan radiography; implications for force and moment generating capacity about the L4/L5 joint. *Journal of Biomechanics* **21**, 329–341.

NARICI, M. V., ROI, G. S. & LANDONI, L. (1988). Force of knee extensor and flexor muscles and cross-sectional area determined by nuclear magnetic resonance imaging. *European Journal of Applied Physiology and Occupational Physiology* **57**, 39–44.

NARICI, M. V., ROI, G. S., LANDONI, L., MINETTI, A. E. & CERRETELLI, P. (1989). Changes in force, cross-sectional area and neural activation during strength training and detraining of the human quadriceps. *European Journal of Applied Physiology and Occupational Physiology* **59**, 310–319.

OTTEN, E. (1988). Concepts and models of functional architecture in skeletal muscle. *Exercise and Sport Sciences Reviews* **16**, 89–138.

REID, J. G. & COSTIGAN, P. A. (1987). Trunk muscle balance and muscular force. *Spine* **12**, 783–786.

REID, J. G., COSTIGAN, P. A. & COMRIE, W. (1987). Prediction of trunk muscle areas and moment arms by use of anthropometric measures. *Spine* **12**, 273–275.

RUGG, S. G., GREGOR, R. J., MANDELBAUM, B. R. & CHIU, L. (1990). *In vivo* moment arm calculations at the ankle using magnetic resonance imaging (MRI). *Journal of Biomechanics* **22**, 495–501.

RYUSHI, T., HÄKKINEN, K., KAUHANEN, H. & KOMI, P. V. (1988). Muscle fibre characteristics, muscle cross-sectional area and force production in strength athletes, physically active males and females. *Scandinavian Journal of Sports Science* **10**, 7–15.

SAMBROOK, P., RICKARDS, D. & CUMMING, W. J. K. (1988). CT muscle scanning in the evaluation of patients with spinal muscular atrophy (SMA). *Neuroradiology* **30**, 487–496.

SAUNDERS, R. D. & SMITH, H. (1984). Safety aspects of NMR clinical imaging. *British Medical Bulletin* **40**, 148–154.

SCHANTZ, P. G., RANDALL-FOX, E., HUTCHINSON, W., TYDÉN, A. & ÅSTRAND, P.-O. (1983). Muscle fibre type distribution, muscle cross-sectional area and maximum voluntary strength in humans. *Acta physiologica scandinavica* **117**, 219–226.

SHAW, D. (1988). The fundamental principles of nuclear magnetic resonance. In *Biomedical Magnetic Resonance Imaging. Principles, Methods and Applications* (ed. F. W. WEHRLI, D. SHAW & J. B. KNEELAND). New York: VCH Publishers.

STUCHLY, M. A. (1990). Application of time-varying magnetic fields in medicine. *Critical Reviews in Biomedical Engineering* **18**, 89–124.

STYTZ, M. R. & FRIEDER, O. (1990). Three-dimensional medical imaging modalities. *Critical Reviews in Biomedical Engineering* **18**, 1–26.

TABATA, I., ATOMI, Y., KANEHISA, H. & MIYASHITA, M. (1990). Effect of high-intensity endurance training on isokinetic muscle power. *European Journal of Applied Physiology and Occupational Physiology* **60**, 254–258.

TRACY, M. F., GIBSON, M. J., SZYPRT, E. P., RUTHERFORD, A. & CORLETT, E. N. (1989). The geometry of the muscles of the lower spine determined by magnetic resonance imaging. *Spine* **14**, 186–193.

WALLACE, W. A. & JOHNSON, F. (1981). Detection and correction of geometrical distortion in X-ray fluoroscopic images. *Journal of Biomechanics* **14**, 123–125.

WANG, J.-Z., MEZRICH, R. S. & SEBOK, D. A. (1990). Image processing on Macintosh II: a practical boundary finding algorithm for biomedical measurement. *Computerized Medical Imaging and Graphics* **14**, 163–171.

WILLAN, P. L. T., MAHON, M. & GOLLAND, J. A. (1990). Morphological variations of the human vastus lateralis muscle. *Journal of Anatomy* **168**, 235–239.

YAMAGUCHI, G. T. & ZAJAC, F. E. (1990). Restoring unassisted natural gait to paraplegics via functional neuromuscular stimulation: a computer stimulation study. *IEEE Transactions on Biomedical Engineering* **37**, 886–902.

YOUNG, A., STOKES, M., ROUND, J. M. & EDWARDS, R. H. T. (1983). The effect of high resistance training on the strength and cross-sectional area of the human quadriceps. *European Journal of Clinical Investigation* **13**, 254–258.

ZHU, X. P., CHECKLEY, D. R., HICKEY, D. S. & ISHERWOOD, I. (1986). Accuracy of area measurements made from MR images compared with computed tomography. *Journal of Computer Assisted Tomography* **10**, 96–102.